Journal of Dental Sciences

Volume 21 | Issue 2 Article 62

2026

Antibacterial tannic acid/polydopamine hybrid coatings for titanium implants

Xu-Fan Yang

Jia-Jia Chung

Chun-Cheng Chen

Shinn-Jyh Ding

Journal of Dental Sciences 21 (2026) 1204–1214

Available online at https://jds.ads.org.tw/journal/

Digital Commons

journal homepage: https://jds.ads.org.tw/journal/

Original Article

Antibacterial tannic acid/polydopamine hybrid coatings for titanium implants

Xu-Fan Yang [a†], Jia-Jia Chung [b†], Chun-Cheng Chen [a,c*], Shinn-Jyh Ding [a,b,c**]

[a] School of Dentistry, Chung Shan Medical University, Taichung City, Taiwan
[b] Institute of Oral Science, Chung Shan Medical University, Taichung City, Taiwan
[c] Department of Stomatology, Chung Shan Medical University Hospital, Taichung City, Taiwan

Received 7 January 2026; Final revision received 27 January 2026
Available online 1 April 2026

KEYWORDS
Titanium;
Dopamine;
Tannic acid;
Antibacterial;
Cytotoxicity

Abstract *Background/purpose:* Bacterial infections pose a significant threat to the longevity of titanium (Ti) implants, often leading to implant failure and peri-implantitis. This study aimed to improve the antibacterial properties of Ti implants by modifying their surfaces with tannic acid (TA) and polydopamine (PDA) as an antibiotic-free strategy.
Materials and methods: Four different concentrations of TA (2, 4, 8, and 16 mg/mL) in Tris buffer served as the deposition solution. TA-based coatings, both with and without the addition of PDA, were applied to Ti substrates via a simple drop-coating approach. The phase composition and microstructure of the coated samples were examined. The antibacterial performance of the coatings against *E. coli* and *S. aureus* was evaluated using various assays. Additionally, the cytotoxicity of the samples was also assessed using L929 cells.
Results: The surface characterization confirmed the successful formation of the coating; however, high concentrations of TA resulted in surface cracking. Importantly, incorporating PDA improved the structural integrity of the hybrid coating without compromising its antibacterial efficacy. Coatings with higher TA loading, specifically 8 mg/mL and 16 mg/mL, effectively eliminated both bacterial strains, achieving a bacteriostatic ratio exceeding 90 %. Furthermore, cytotoxicity assays demonstrated good cytocompatibility for all coatings, although a slight decline in cell viability was observed with increasing TA concentration.
Conclusion: This study highlighted that the coating formulated with 8 mg/mL TA in combination with PDA provided an optimal balance between antibacterial efficacy, structural integrity, and cytocompatibility. This cost-effective and straightforward coating showed promising potential for use in antibacterial titanium implants.

* Corresponding author. School of Dentistry, Chung Shan Medical University, No. 110, Sec. 1, Jianguo N. Road, Taichung City, 40201, Taiwan.
** Corresponding author. Institute of Oral Science, Chung Shan Medical University, No. 110, Sec.1, Jianguo N. Rd., Taichung City, 40201, Taiwan.
E-mail addresses: fw3256@gmail.com (C.-C. Chen), sjding@csmu.edu.tw (S.-J. Ding).
† These authors contributed equally to this work.

https://doi.org/10.1016/j.jds.2026.01.025

Introduction

Titanium (Ti) and its alloys have been widely used as metal implants in orthopedic and dental applications for years owing to their favorable biocompatibility, excellent mechanical properties, and high wear resistance.[1—3] However, the challenge remains that pristine Ti implants lack intrinsic antibacterial properties, rendering them vulnerable to bacterial contamination after implantation.[4—6] This susceptibility leads to bacterial adhesion and subsequent biofilm formation on implant surfaces, which can trigger peri-implant infections, promote osteoclast differentiation, and lead to progressive bone loss around the implant.[7] These complications ultimately lead to implant failure due to mechanical instability and poor osseointegration.[6,8] A recent systematic review and meta-analysis revealed alarming statistics: the prevalence of peri-implantitis stands at 19.53 % at the patient level and 12.53 % at the implant level,[9] underscoring the urgent need for improved implant surface designs to mitigate infection-related complications. In response, extensive efforts have been devoted to modifying Ti implant surfaces to enhance antibacterial performance through physical and chemical approaches, thereby improving implant longevity and reducing complications.[10—12]

Antibiotics are commonly used to prevent or treat infections.[13] However, once a mature biofilm is formed, bacteria become highly resistant, making eradication difficult even at high concentrations of antibiotics.[14,15] Moreover, increasing restrictions on antibiotic use due to the growing threat of antibiotic resistance pose significant challenges to infection control.[16] To this end, antibiotic-free antibacterial materials have emerged as promising alternatives to conventional antibiotics.[17,18] Among these alternatives, polyphenols— a large class of plant-derived secondary metabolites— have gained considerable attention due to their broad-spectrum antimicrobial, antioxidant, and anti-inflammatory properties, along with favorable cytocompatibility.[19—21] Among this class, high-molecular-weight and hydrolysable tannic acid (TA) is particularly favorable for localized antibacterial applications compared to other polyphenolic compounds.[21,22] In contrast, many low-aqueous-solubility polyphenols, particularly flavonoids, have limited therapeutic use due to the difficulties in dissolving into physiological fluids.[23] In addition, TA possesses a high density of phenolic hydroxyl groups that enable versatile interactions with other functional groups through hydrogen bonding under mild conditions, facilitating the formation of stable complexes with enhanced functionalities.[24] For instance, research by Zhou et al. demonstrated the potential of curdlan-tannic acid hybrid hydrogels, which not only exhibited antibacterial, antioxidant, and hemostatic activities, but also maintained good cytocompatibility and accelerated wound healing in vivo.[25] Despite the increasing interest in TA—based antibacterial coatings, several challenges remain unresolved. Systematic investigations defining an optimal TA concentration for Ti implant surfaces are limited.[26] These coatings often exhibit concentration-dependent behavior, where higher TA levels enhance antibacterial efficacy but may simultaneously increase risks related to cytocompatibility or coating integrity.[27,28] This inherent trade-off among antibacterial performance, cytocompatibility, and coating stability has been recognized as a major design concern for implant-related applications. Moreover, due to its water solubility and predominantly non-covalent interactions with metallic substrates, TA coatings may suffer from limited surface stability and potentially uncontrolled release, which could raise concerns about biological responses.[29,30] These limitations consistently indicate the necessity of an interfacial agent that can improve coating stability while preserving antibacterial efficacy and biocompatibility.

Polydopamine (PDA), a mussel-inspired adhesive polymer, has emerged as a powerful tool in biomaterials owing to its facile deposition on diverse surfaces and its reactive functional groups.[31,32] Its monomers contain both catechol and amine groups, enabling self-polymerization and interactions with molecules, such as TA, through mechanisms like hydrogen bonding, $\pi-\pi$ stacking, Michael addition, and Schiff base reactions under alkaline environments.[33,34] Feng et al. reported that PDA functioned as an interfacial molecular bridge in nano-hydroxyapatite/polycaprolactone composite scaffolds, enhancing the tensile and compressive strength by 10 % and 16 %, respectively.[35] Additionally, PDA has demonstrated excellent biocompatibility and strong tissue adhesion, with no noticeable cytotoxic effects.[10,36] Liu et al. further demonstrated that PDA-coated gold nanoparticles formed ultra-stable coatings in vivo, showing low cytotoxicity, efficient cellular uptake, and negligible long-term histological toxicity in various organs.[37] Accordingly, PDA have been widely recognized as an effective interfacial adhesive for surface modification of antibacterial agents and biological materials, achieving clinical applications.

Composite coating strategies have therefore been explored to overcome the limitations of single-component systems. Notably, TA and PDA possess complementary physicochemical properties, and their functional groups enable strong interfacial interactions with titanium substrates. Previous studies on PDA-assisted or polyphenol-based antibacterial coatings have demonstrated promising antibacterial performance, often through increased agent loading, incorporation of additional antibacterial components, or multi-step surface modification processes.[30,38] However, such strategies may raise concerns regarding coating complexity, cytocompatibility, or practical applicability for implant surfaces. Recently, a limited number of studies have explored the application of TA/PDA complexes for antifouling reverse osmosis membranes and for targeted

bacterial elimination through nanorobotic or implant-related systems.[38–40] These existing studies primarily emphasize antibacterial or antifouling performance using a fixed coating formulation, with limited investigation of concentration-dependent effects or direct comparisons between polyphenol-only and PDA-assisted systems. As a result, the role of PDA in stabilizing polyphenol coatings and in modulating the trade-off between antibacterial activity and cytocompatibility remains insufficiently understood. Therefore, this study aimed to investigate the concentration effect of TA and TA/PDA hybrid coatings on Ti substrates. By varying the TA loading with or without PDA incorporation, the coating morphology, chemical composition, antibacterial activity, and cytotoxicity were comprehensively evaluated. Moreover, the optimal balance between antibacterial performance and biocompatibility required for dental implant applications can be clearly established.

Materials and methods

Substrate preparation

Titanium plates (Spemet Co., Taipei, Taiwan) were cut into $10 \times 10 \times 3$ mm^3 pieces, which served as the substrates. Each piece was polished with #400 and #1500 grit silicon carbide sandpapers. After polishing, the pieces were cleaned with acetone and ethanol in an ultrasonic vibrator for 15 min, rinsed with deionized water, and dried in a 37 °C oven.

Coating preparation

To prepare a PDA sample, 100 mg of dopamine (Sigma—Aldrich, St. Louis, MO, USA) was dissolved in 50 mL of 10 mM tris(hydroxymethyl)aminomethane solution (Tris buffer; pH 8.5), resulting in a 2 mg/mL solution. Subsequently, 100 μL of this dopamine solution was applied to the titanium plate and then heated in an oven at 60 °C for 24 h. Tannic acid (Alfa Aesar, Heysham, England) was added to the Tris buffer in varying amounts to create four different samples with concentrations of 2, 4, 8, and 16 mg/mL, referred to as TA2, TA4, TA8, and TA16, respectively. For composite coatings with different TA/PDA ratios, the TA powder was blended into the dopamine solution, forming groups DTA2, DTA4, DTA8, and DTA16. All coatings were prepared in a single deposition cycle under mild shaking, and their sample codes are listed in Table 1.

Table 1 Coating sample codes along with their corresponding formulas.

Sample codes	DA (mg/mL)	TA (mg/mL)
TA2	0	2
TA4	0	4
TA8	0	8
TA16	0	16
PDA	2	0
DTA2	2	2
DTA4	2	4
DTA8	2	8
DTA16	2	16

DA, dopamine; TA, tannic acid.

Surface composition and morphology

The phase composition of the sample surface was analyzed using high-resolution X-ray diffraction (HR-XRD; D8 SSS, Bruker, Karlsruhe, Germany) with CuKα radiation over a 2θ range of 20—45° at a scan speed of 1°/min. To further investigate the chemical structures, the samples were examined using Fourier transform infrared spectroscopy (FTIR; Vertex 80v, Bruker, Ettlingen, Germany) over a wavenumber range of 500—2000 cm^{-1}. Moreover, the surface and cross-sectional micromorphology of the samples were examined after gold coating using a scanning electron microscope (SEM; JSM-7800F, JEOL, Tokyo, Japan).

Bacterial culture

Gram-negative *Escherichia coli* (*E. coli*; ATCC 8739, Hsinchu, Taiwan) and Gram-positive *Staphylococcus aureus (S. aureus*; ATCC 25923, Hsinchu, Taiwan) were used to test antibacterial effectiveness, with a coating-free Ti sample as a negative control. After sterilization with ultraviolet light for 30 min, each sample was placed in 1 mL of tryptic soy broth (Becton Dickinson, Sparks, MD, USA) containing either 10^7 or 10^4 colony-forming units (CFU)/mL of bacteria for 3 or 24 h at 37 °C, respectively. Samples with bacterial attachment were then transferred to new culture plates for further analysis.

AlamarBlue assay

The number of viable bacteria was measured by the redox reaction between the alamarBlue colorimetric indicator dye and the active bacteria.[5] After culture, each sample was treated with a tenfold diluted alamarBlue (Invitrogen, Grand Island, NY, USA) and incubated for 30 min at 37 °C. Absorbance was measured at 570 nm and 600 nm using a BioTek Epoch microplate reader (Winooski, VT, USA) to calculate the bacteriostatic ratio (%).[41] Three samples from each group were analyzed.

Spread plate method

The traditional agar plate method was utilized to quantify bacterial colonies and evaluate antibacterial effects. After culturing for 3 and 24 h, the samples were placed in 1 mL PBS in culture plates and subjected to ultrasonic vibration for 5 min to detach the adhered bacteria from the samples. A 100 μL bacterial suspension was serially diluted tenfold with PBS and spread on a 15 mL Trypticase soy agar plate. After 24 h of incubation, CFUs in each Petri dish were counted to calculate the bacteriostatic ratio using the following equation: Bacteriostatic ratio (%) = (number of Ti control - number of samples)/number of Ti control × 100 %.[42]

Morphology observation of bacteria

To observe bacterial colonies on different surfaces, samples were fixed in 4 % paraformaldehyde (Sigma–Aldrich) for 20 min after a 24-h culture period. They were then dehydrated for 20 min at each concentration using a graded series of ethanol before being mounted on a sample stage and coated with gold. This preparation was done to enable observation under a SEM.

L929 cytotoxicity

A mouse fibroblast cell line (L929) was selected for testing cytotoxicity. Samples were sterilized with UV light for 30 min and then placed in culture plates containing 10^4 L929 cells per well. Dulbecco's modified Eagle medium (DMEM; Gibco, Langley, OK, USA) was used, supplemented with 10 % fetal bovine serum and 1 % penicillin/streptomycin solution. After culturing for 12, 24, and 48 h at 37 °C, an alamarBlue assay was performed to assess cell viability. Absorbance values measured with a BioTek Epoch spectrophotometer were used to calculate cell viability (%), normalized against the Ti control.[10]

Statistical analysis

One-way ANOVA and Duncan's post-hoc test were used to compare the means of the samples. If $P < 0.05$, there is a significant difference between the conditions.

Results

Phase and chemical composition

The phase compositions of the samples were characterized using XRD, as illustrated in Fig. 1a. The diffraction peaks at $2\theta = 35.1°$, $38.4°$, and $40.1°$ corresponded to the (100), (002), and (101) crystal planes of the Ti substrate, respectively.[10] In the samples coated with TA, no distinct crystalline peaks were detected. However, with increasing TA concentration, a broad feature around $2\theta = 25.2°$ became more pronounced, particularly in the TA16 and DTA16, indicating the presence of an amorphous structure of TA.[43] Additionally, the incorporation of PDA did not induce any additional crystalline phases, confirming that the PDA modification did not alter the crystalline structure of the coatings.[10,42]

To differentiate the phase composition among the Ti substrate, TA-coated samples, and PDA-modified samples, FTIR analysis was employed, as shown in Fig. 1b. The TA-coated samples showed distinct absorption bands at 1716, 1614, 1534, 1449, 1354, 1229, 1086, 1037, 871, and 757 cm^{-1}, all of which were indicative of tannic acid and consistent with previous findings.[44] The 1716 cm^{-1} band corresponded to the C]O stretching of free gallic acid. The 1614 and 1449 cm^{-1} bands related to aromatic C]C stretching and C–H bending vibrations of the aromatic ring, while the band at 1534 cm^{-1} was attributed to the symmetric stretching vibrations of aromatic C]C bonds.[44] The band at 1354 cm^{-1}, corresponding to C–O–C stretching and

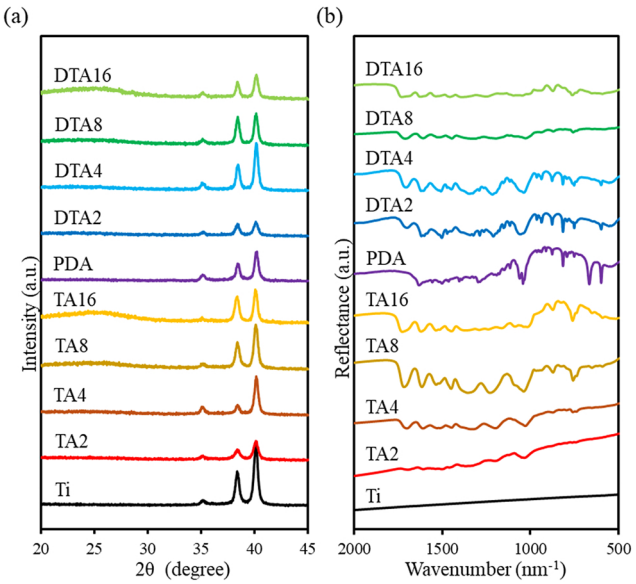

Figure 1 (a) X-ray diffraction patterns and (b) Fourier transform infrared spectra of all samples.

O–H deformation vibrations, indicated the presence of hydrolysable tannins. The band near 1229 cm^{-1} was assigned to the stretching vibrations of C–O bonds in polyols, and the absorption at approximately 1037 cm^{-1} was attributed to the C–O–C bending mode. Furthermore, the appearance of characteristic bands at 1086 cm^{-1} (aryl phenolic ester C–O–C symmetric stretching), 871 cm^{-1} (C–C stretching), and 757 cm^{-1} (sugar ring breathing vibration) allowed for the explicit identification of these hydrolysable tannins as gallotannins.[45] For PDA, key bands at 1631, 1519, and 1115 cm^{-1} were assigned to amine N–H bending, aromatic C]C stretching, and ester C–O stretching vibrations, respectively.[46] While DTA hybrid groups displayed absorption bands from both TA and PDA, no additional bands were detected. Furthermore, in samples with a high TA content, the PDA-related bands became less pronounced, rendering the spectra of DTA16 similar to that of TA16.

Coating morphology

The surface and cross-sectional morphologies of the samples were examined by SEM, as depicted in Fig. 2a and b, respectively. In comparison to the pristine Ti surface, which exhibited rough grooves, the TA-coated samples demonstrated noticeably smoother surfaces (Fig. 2a). This can be attributed to the formation of a gel-like TA layer covering the substrate. However, excessive TA concentrations led to surface cracking, particularly in the TA16 sample. In contrast, the addition of polydopamine (PDA) to high-concentration TA coatings effectively prevented crack formation, with no visible cracks on the DTA16 coating. Regarding the PDA sample, small particulate features were visible on its surface. In contrast, such features were absent on the DTA hybrid coatings, which retained a smooth texture similar to that of the TA-coated samples. In the cross-sectional view (Fig. 2b), all coatings exhibited a

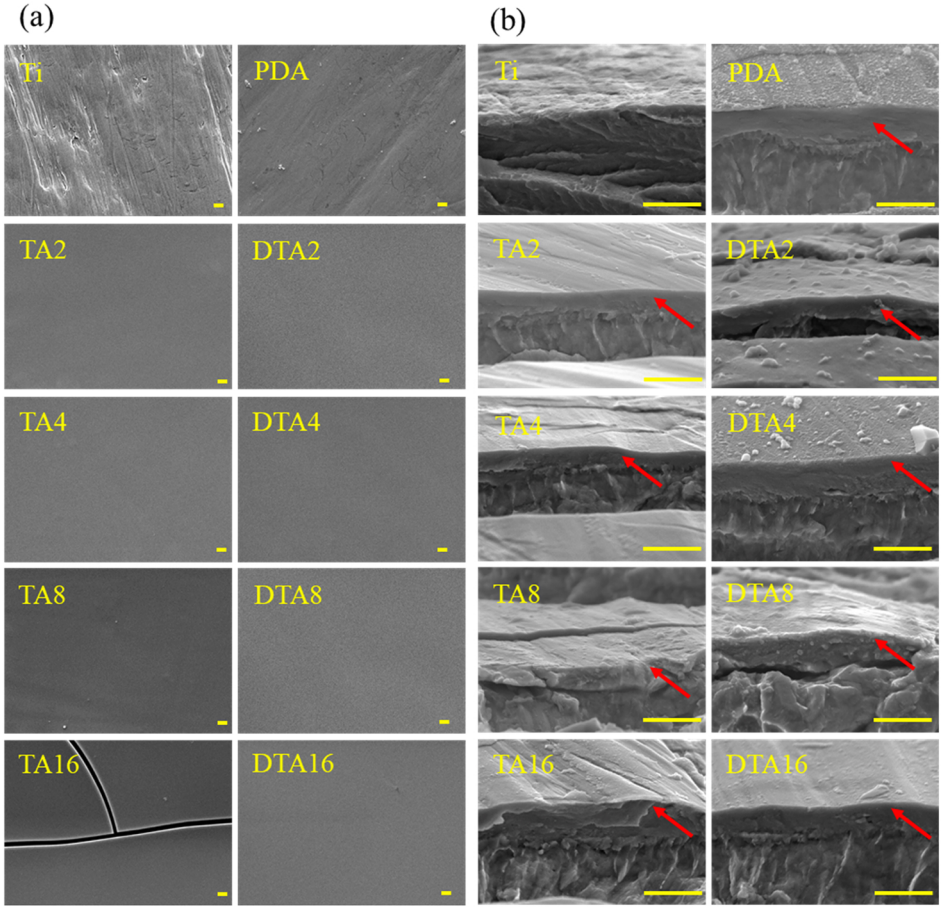

Figure 2 (a) Surface and (b) cross-sectional scanning electron microscope images of all samples. The arrows indicate the coating on the substrate in cross-sectional view. Scale bar, 1 μm.

notably smooth structure, which contrasted with the plastic deformation of the Ti substrate. Notably, the coating thickness was approximately 300 nm across all coating samples, regardless of the TA concentration.

Antibacterial ability detected by alamarBlue assay

To evaluate the antibacterial performance of various samples, the bacteriostatic ratio (%) against *E. coli* (Fig. 3a) and *S. aureus* (Fig. 3b) was determined. When normalized to the Ti control, TA2 demonstrated a low antibacterial effect, achieving only 26 % inhibition against *E. coli* after a short incubation period of 3 h (Fig. 3a). In contrast, TA4 showed a high bacteriostatic ratio of 78 % during the identical short incubation; however, this value dropped to 40 % after prolonged incubation of 24 h. Coating samples with higher TA concentrations, specifically TA8 and TA16, achieved almost complete bacterial elimination against *E. coli* at both short and long incubation times, with no significant difference in their effectiveness ($P > 0.05$). Regarding the PDA sample, it exhibited limited antibacterial ability. Accordingly, DTA-modified samples presented comparable antibacterial efficiencies to those of their corresponding TA-only counterparts, indicating that TA was the dominant component responsible for antibacterial activity. A comparable trend was observed with *S. aureus* (Fig. 3b), regardless of the incubation time. For instance, after 24 h of incubation, DTA2, DTA4, and DTA8 exhibited bacteriostatic ratios of 21 %, 38 %, and 93 % against *E. coli*, respectively (Fig. 3a). The corresponding ratios against *S. aureus* were 38 %, 50 %, and 94 % (Fig. 3b), confirming that higher TA concentrations were effective against both Gram-negative and Gram-positive bacteria. Notably, the coatings prepared from 8 to 16 mg/mL TA demonstrated more effective antibacterial activity, achieving bacteriostatic ratios exceeding 90 %.

Antibacterial ability detected by the spread plate method

The bactericidal performance could be directly seen from the agar plate images cultured with *E. coli* (Fig. 4a) and *S. aureus* (Fig. 4b). Compared to the Ti control, samples containing a high content of TA, namely TA8, TA16, DTA8, and DTA16, exhibited almost no visible bacterial colonies after 24 h of incubation, indicating TA effectively enhanced antibacterial activity against both Gram-negative or -positive bacteria. The CFUs were further quantified and normalized to the Ti control, and the results against *E. coli* and *S. aureus* are shown in Fig. 4c and d, respectively. Samples with a high TA content maintained nearly 100 % bacteriostatic ratio at both short and long incubation times

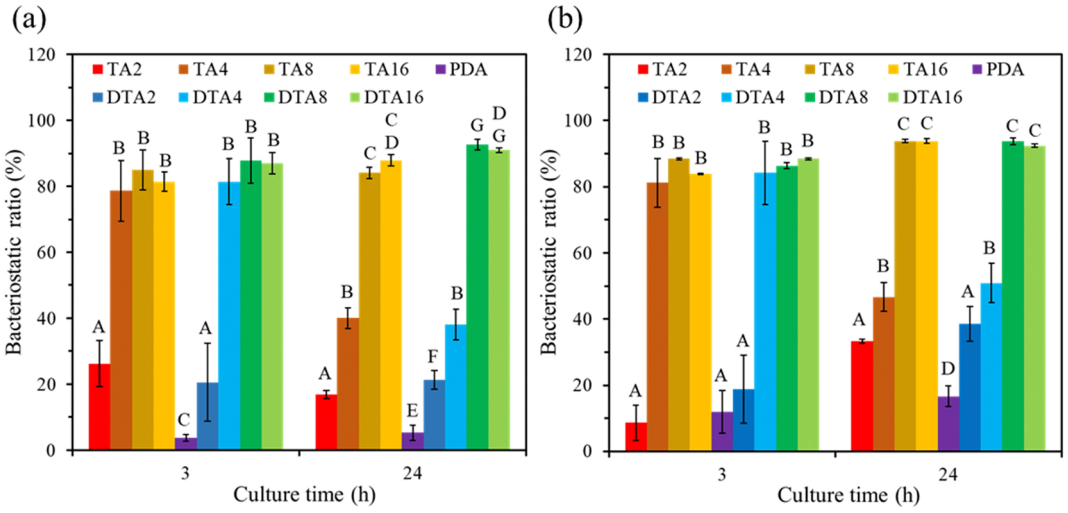

Figure 3 Alamar blue assay for bacteriostatic ratio (%) of various samples against (a) *E. coli* and (b) *S. aureus* after both short-term (3 h) and long-term (24 h) incubation. The Ti control serves as a reference. Statistical comparisons were made among samples at the same time point. Different capital letters indicate significant differences at $P < 0.05$ (n = 3).

against *E. coli* (Fig. 4c). In contract, pure PDA and samples with a low TA content, namely TA2, TA4, DTA2, and DTA4, displayed bacteriostatic ratios below 60 % after long-term incubation, although TA4 and DTA4 temporarily reached nearly complete bacterial inhibition at the short incubation time. A similar antibacterial trend was observed against *S. aureus* (Fig. 4d), where only samples with sufficient TA, such as TA8 and TA16, as well as DTA8 and DTA16, were able to sustain effective bacterial elimination over prolonged incubation.

Bacterial colony observation

SEM observations were employed to further confirm bacterial colonization on different coating surfaces after 24 h of incubation, as shown in Fig. 5. The Ti substrate and pure PDA coating exhibited excessive spreading of rod-shaped *E. coli* (Fig. 5a). In contrast, TA-coated samples, with or without PDA, showed a reduced number of bacteria, demonstrating the effectiveness of the coatings. Similarly, spherical *S. aureus* also densely aggregated on Ti and PDA surfaces (Fig. 5b), but bacterial adhesion decreased with increasing TA content. Significantly, a comparison between TA and DTA coatings revealed that the incorporation of PDA did not compromise the antibacterial performance.

Cytotoxicity

The cytotoxicity of antibacterial materials is a critical consideration for biomedical applications; therefore, the viability of L929 cultured on various coating samples was evaluated. As shown in Fig. 6, all samples exhibited viabilities exceeding 70 % at all culture time points, indicating no cytotoxicity effects, as per ISO 10993-5 standards. The PDA sample maintained a viability range of 90–100 % throughout the incubation period, comparable to that of the Ti control, suggesting the PDA layer did not impact cell viability. It was also observed that cell viability exhibited a slight concentration-dependent decrease at each time point of culture. For instance, after 12 h of incubation, the viabilities for TA2, TA4, TA8, and TA16 were 89 %, 83 %, 82 % and 80 %, respectively. Similarly, the viabilities for DTA2, DTA4, DTA8, and DTA were 87 %, 82 %, 80 %, and 78 %, respectively, indicating no significant differences ($P > 0.05$). Notably, at the same TA concentration, the coatings with and without PDA displayed similar cell viabilities. After 24 h of incubation, there were no significant differences in cell viability among the TA-containing coatings, except for the PDA coating. When culturing for 48 h, the coatings with higher TA content, such as TA8, TA16, as well as DTA8 and DTA16, demonstrated viability of over 80 %.

Discussion

Tannic acid is widely recognized as a broad-spectrum antimicrobial agent effective against both Gram-positive and Gram-negative bacteria, and it has been incorporated into various biomedical materials.[44,47] In this study, we evaluated the antibacterial performance of TA across different concentrations through a series of assays, including the alamarBlue assay, spread plate method, and SEM observation, following physicochemical evaluations. FTIR and XRD analyses of the coatings confirmed that the crystalline structure of the underlying Ti substrate was preserved after surface modification. These findings, together with the SEM observations, demonstrated the successful deposition of TA and PDA on the Ti substrates. Consistent with previous studies employing PDA as an interfacial adhesive layer,[10,48,49] the incorporation of PDA in this study aimed to enhance the adhesion and structural stability of the coating. The SEM surface observations revealed that the TA16 coatings developed visible surface cracks, likely due to the accumulation of internal stress at high coating concentrations.[50] In stark contrast, such cracks appeared to be reduced in the DTA16 coatings, indicating that the presence of PDA effectively improved coating

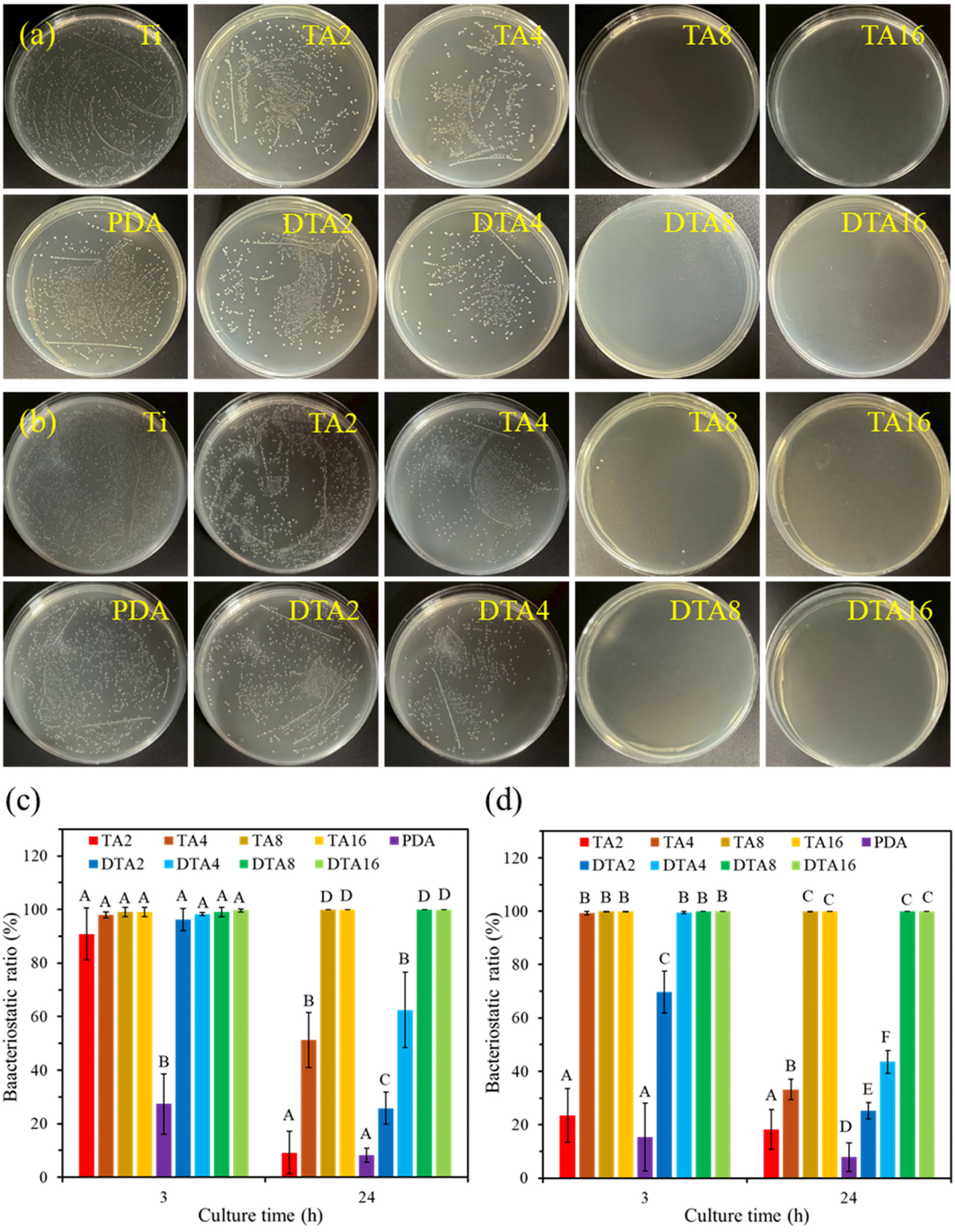

Figure 4 Representative images of agar plate tests for (a) *E. coli* and (b) *S. aureus* bacteria after culturing on sample surfaces for 24 h. The corresponding bacteriostatic ratios (%) for various samples are presented for both 3-h and 24-h seeding times. The Ti control serves as a reference. Different capital letters indicate statistically significant differences at the same time point when $P < 0.05$ (n = 3).

cohesion and alleviated internal stress within the coating layer.

The results of antibacterial assays indicated a slight concentration-dependent effect of TA against both *E. coli* and *S. aureus*, in agreement with previous studies.[28,44,51] For example, Winiecki et al. reported similar antibacterial trends when evaluating TA coatings on plasma-activated Ti surfaces against *E. coli*, *S. aureus*, and *P. aeruginosa* using culture plate analysis and live/dead staining.[28] Across all antibacterial evaluation methods employed in this study, a consistent pattern emerged: coatings with lower TA concentrations, such as TA4, were insufficient to eliminate most bacterial populations. In contrast, higher TA concentrations, such as TA8, exhibited a remarkably enhanced bacteriostatic effect, which was further sustained or improved at TA16. Unlike earlier studies that relied on low

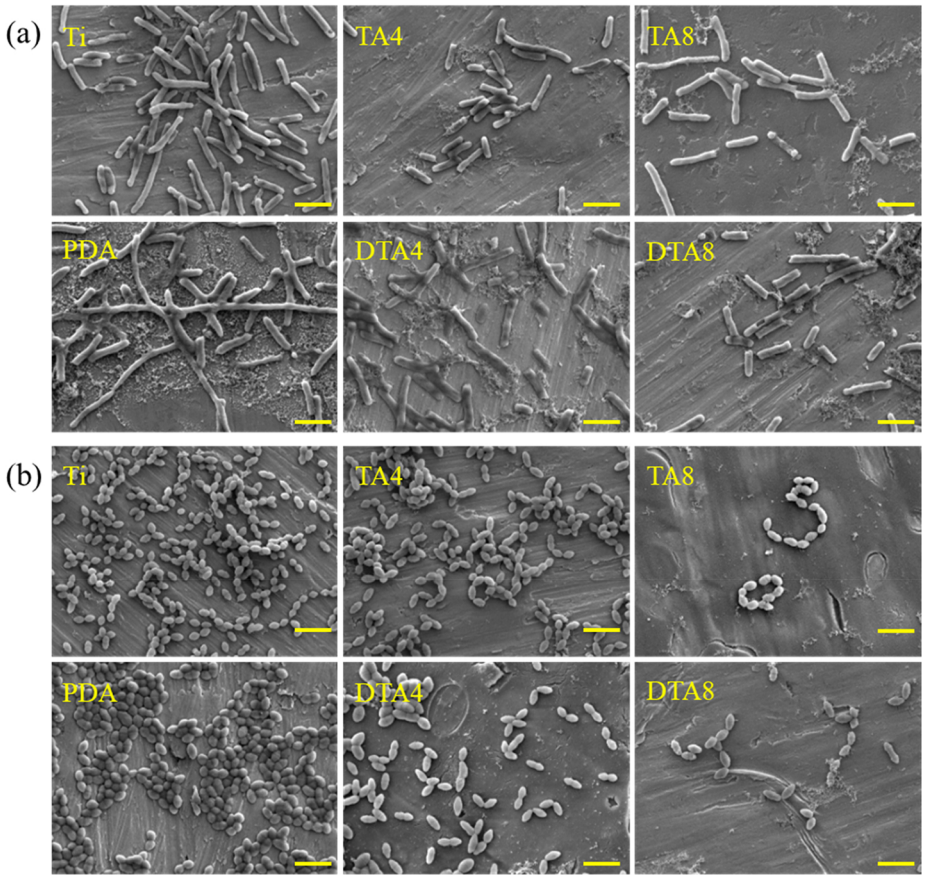

Figure 5 Scanning electron microscope images of (a) *E. coli* and (b) *S. aureus* on the surfaces of Ti, TA200, TA400, DA, DT200, and DT400 showing bacterial adhesion after 24 h of incubation. Scale bar, 3 μm.

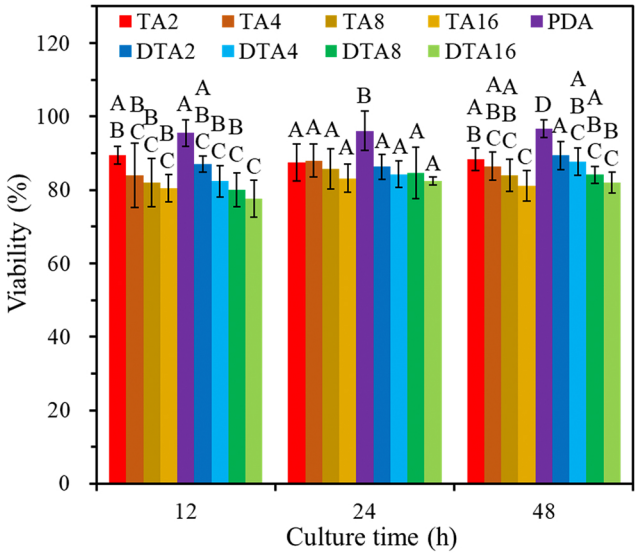

Figure 6 Cytotoxicity evaluation of various samples cultured with L929 cells at different time points. Statistical comparisons were made between the samples at the same time point. Different capital letters indicate statistically significant differences ($P < 0.05$, n = 3). Cell viability was normalized to the Ti control.

TA concentrations (e.g., 2 mg/mL) that necessitated the addition of other antibacterial agents for adequate efficacy,[40,52] our findings demonstrated that a sufficient amount of TA on its own could produce notable antibacterial activity. Furthermore, a comparison of short-term (3 h) and long-term (24 h) antibacterial effects revealed a concerning trend: samples with inadequate TA, such as TA4, showed diminished bacteriostatic ratios over extended time periods. Kaczmarek-Szczepańska et al. reported that tannic acid release from titanium surfaces decreased over time and that the concentration of released TA depended on the initial TA concentration deposited on the surface.[53] This release behavior may explain the reduced antibacterial effectiveness observed in our study at longer incubation times, as an initially high local TA concentration could be generated during the early stage and gradually diminish over time. If the initial antibacterial challenge failed to eradicate most bacteria, the surviving viable bacteria could proliferate, leading to reduced antibacterial effectiveness over longer durations. Conversely, TA8 achieved near-complete bacterial elimination after 24 h, showing no significant difference in effectiveness compared to TA16.

When examining the hybrid coatings, the antibacterial results consistently showed no significant differences between the PDA-modified samples and their corresponding TA samples. This suggested that PDA itself contributed minimally to the antibacterial properties, while TA

dominated the antibacterial behavior of the hybrid coatings. This observation was consistent with previous studies, which noted that PDA primarily functioned as an adhesive layer and generally required a combination with additional antibacterial agents, such as metal ions or peptides, to exert practical antibacterial effects.[42,46] Mechanistically, TA has been shown to interact with bacterial cell membranes, bind to surface proteins and enzymes,[47] and reduce bacterial adhesion.[54] These interactions disrupt essential cellular functions, ultimately leading to the inactivation of bacteria.[55] In our study, the concentration-dependent reduction in bacterial metabolic activity, as measured by the alamarBlue assay, was further corroborated by a corresponding decrease in viable colony counts from the spread plate assay. For *S. aureus* cultured for 24 h, the bacteriostatic ratios measured by the alamarBlue assay were approximately 15 %, 40 %, 50 %, 90 %, and 90 % for the PDA, DTA2, DTA4, DTA8, and DTA16 samples, respectively. Similarly, the corresponding CFU counting was approximately 10 %, 25 %, 45 %, and near-complete elimination for the DTA8 and DTA16 samples. The comparable concentration-dependent trends observed across methods provide conceptual cross-validation of the antibacterial performance of the coatings. Additionally, SEM observations revealed a reduction in bacterial adhesion on the coated sample surfaces. Collectively, these findings reflected the effective antibacterial activity of the hybrid coatings.

Biocompatibility is a crucial consideration for biomedical surface applications. Our cytotoxicity evaluations using L929 fibroblasts revealed that TA-coated and those incorporating PDA exhibited no apparent adverse effects on cell viability, with all values surpassing the 70 % threshold defined by ISO 10993-5 standards. Notably, the cell viability associated with these coatings exhibited an inverse dose-dependent response to TA, indicating that TA possessed good biocompatibility, which was consistent with previous studies.[28,56] For example, Yang et al. demonstrated that TA reduced the viability of H9C2 cells in a dose-dependent manner within the range of 0—50 μM.[56] Importantly, it is recognized that excessively high coating concentrations may elevate the risk of undetectable defects. Therefore, it became clear that a PDA-enhanced intermediate TA concentration, such as the DTA8 coating, was considered more favorable for achieving a balanced performance due to its coating integrity, antibacterial properties, and cytocompatibility. Compared to previous complicated methods, such as layer-by-layer and encapsulation techniques,[30,38] the current TA/PDA coating developed here can be fabricated through a simple and mild preparation process, while enabling systematic modulation of antibacterial performance, cytocompatibility, and surface structure.

In conclusion, our findings indicated that TA-based coatings, with and without PDA, were successfully applied to Ti substrates. Results from multiple antibacterial assays consistently demonstrated that coatings with a sufficiently high concentration of TA effectively eliminated bacteria even after prolonged incubation periods. The cytotoxicity evaluation revealed no apparent adverse effects on cell viability, with all coated samples showing over 70 % when normalized to the Ti control. Notably, while PDA did not significantly influence antibacterial efficacy, its incorporation markedly improved the structural integrity of the hybrid coatings by reducing crack formation. Among the tested coatings, the formulation containing 8 mg/mL TA combined with PDA (designated as DTA8) exhibited the most favorable performance, achieving effective antibacterial activity while maintaining coating integrity and cytocompatibility. This antibiotic-free antibacterial coating holds promising potential for the surface modification of Ti implants, aiming to reduce the risk of implant-associated infections.

Declaration of competing interest

The authors have no conflicts of interest relevant to this article.

Acknowledgments

This work was supported by a research grant (NSTC 113-2813-C-040-062-B) from the National Science and Technology Council, Taiwan. We sincerely appreciate Ya-Hsun Lin (the Instrument Centre of National Chung Hsing University, NSTC 113-2740-M-005-001) and Ti-Yi Lu (the Instrumentation Center of National Tsing Hua University, NSTC 113-2740-M-007-001) for their help with FESEM and FTIR measurements, respectively.

References

1. Geetha M, Singh AK, Asokamani R, Gogia AK. Ti based biomaterials, the ultimate choice for orthopaedic implants — a review. *Prog Mater Sci* 2009;54:397—425.
2. Nicholson JW. Titanium alloys for dental implants: a review. *Prosthesis* 2020;2:100—16.
3. Cheng YH, Chen CC, Ding SJ. Unveiling the characteristics and surface modification of titanium, zirconia, and polyetheretherketone dental implants. *J Dent Sci* 2025;20:2046—57.
4. Fürst MM, Salvi GE, Lang NP, Persson GR. Bacterial colonization immediately after installation on oral titanium implants. *Clin Oral Implants Res* 2007;18:501—8.
5. Tsai CF, Chung JJ, Ding SJ, Chen CC. In vitro cytotoxicity and antibacterial activity of hypochlorous acid antimicrobial agent. *J Dent Sci* 2024;19:345—56.
6. Pye AD, Lockhart DEA, Dawson MP, Murray CA, Smith AJ. A review of dental implants and infection. *J Hosp Infect* 2009;72:104—10.
7. Fernandes M, Gomes P. Bone cells dynamics during peri-implantitis: a theoretical analysis. *J Oral Maxillofac Res* 2016;7:e6.
8. Sakka S, Baroudi K, Nassani MZ. Factors associated with early and late failure of dental implants. *J Investig Clin Dent* 2012;3:258—61.
9. Diaz P, Gonzalo E, Villagra LJG, Miegimolle B, Suarez MJ. What is the prevalence of peri-implantitis? A systematic review and meta-analysis. *BMC Oral Health* 2022;22:449.
10. Kao H, Chen CC, Huang YR, Chu YH, Csik A, Ding SJ. Metal ion-dependent tailored antibacterial activity and biological properties of polydopamine-coated titanium implants. *Surf Coat Technol* 2019;378:124998.
11. Xue T, Attarilar S, Liu S, et al. Surface modification techniques of titanium and its alloys to functionally optimize their biomedical properties: thematic review. *Front Bioeng Biotechnol* 2020;8:603072.

12. Sun XD, Liu TT, Wang QQ, Zhang J, Cao MS. Surface modification and functionalities for titanium dental implants. *ACS Biomater Sci Eng* 2023;9:4442–61.
13. Jayaraman S. Interventions for replacing missing teeth: antibiotics in dental implant placement to prevent complications: evidence summary of Cochrane review. *J Indian Prosthodont Soc* 2015;15:179–82.
14. Yan J, Bassler BL. Surviving as a community: antibiotic tolerance and persistence in bacterial biofilms. *Cell Host Microbe* 2019;26:15–21.
15. Di Domenico EG, Rimoldi SG, Cavallo I, et al. Microbial biofilm correlates with an increased antibiotic tolerance and poor therapeutic outcome in infective endocarditis. *BMC Microbiol* 2019;19:228.
16. Llor C, Bjerrum L. Antimicrobial resistance: risk associated with antibiotic overuse and initiatives to reduce the problem. *Ther Adv Drug Saf* 2014;5:229–41.
17. Wang Y, Yang Y, Shi Y, Song H, Yu C. Antibiotic-free antibacterial strategies enabled by nanomaterials: progress and perspectives. *Adv Mater* 2020;32:1904106.
18. Akshaya S, Rowlo PK, Dukle A, Nathanael AJ. Antibacterial coatings for titanium implants: recent trends and future perspectives. *Antibiotics (Basel)* 2022;11:1719.
19. Daglia M. Polyphenols as antimicrobial agents. *Curr Opin Biotechnol* 2012;23:174–81.
20. Singh A, Yau YF, Leung KS, El-Nezami H, Lee JC. Interaction of polyphenols as antioxidant and anti-inflammatory compounds in brain-liver-gut axis. *Antioxidants (Basel)* 2020;9:669.
21. Aatif M. Current understanding of polyphenols to enhance bioavailability for better therapies. *Biomedicines* 2023;11:2078.
22. Hagerman AE, Riedl KM, Jones GA, et al. High molecular weight plant polyphenolics (tannins) as biological antioxidants. *J Agric Food Chem* 1998;46:1887–92.
23. Hashim NT, Babiker R, Padmanabhan V, et al. Polyphenolic compounds in combating MDR periodontal pathogens: current research and future directions. *Front Pharmacol* 2025;16:1678979.
24. Hosseini M, Moghaddam L, Barner L, Cometta S, Hutmacher DW, Medeiros Savi F. The multifaceted role of tannic acid: from its extraction and structure to antibacterial properties and applications. *Prog Polym Sci* 2025;160:101908.
25. Zhou Z, Xiao J, Guan S, Geng Z, Zhao R, Gao B. A hydrogen-bonded antibacterial curdlan-tannic acid hydrogel with an antioxidant and hemostatic function for wound healing. *Carbohydr Polym* 2022;285:119235.
26. Ding X, Zhang G, Yiu CKY, Li X, Shan Z. Unleashing the potential of tannic acid in dentistry: a scoping review of applications. *Bioengineering (Basel)* 2025;12:438.
27. Zhang W, Zhang Y, Li X, et al. Multifunctional polyphenol-based silk hydrogel alleviates oxidative stress and enhances endogenous regeneration of osteochondral defects. *Mater Today Bio* 2022;14:100251.
28. Winiecki M, Stepczyńska M, Walczak M, et al. Antibacterial and antifungal tannic acid coating on plasma-activated titanium alloy surface. *Int J Mol Sci* 2025;26:7051.
29. Lin N, Wang L, Tang H, et al. Co-deposition of tannic acid and bottle-brush polymer to construct stable antifouling surface via hydrogen-bonding. *Surf Interfaces* 2024;53:105010.
30. Oreja E, Zaytseva-Zotova D, Rogala A, et al. Multifunctional tannic acid and polyamino acid layer-by-layer coatings for tailored implant surfaces. *ACS Biomater Sci Eng* 2025;11:5376–88.
31. Ho CC, Ding SJ. Structure, properties and applications of mussel-inspired polydopamine. *J Biomed Nanotechnol* 2014;10:3063–84.
32. Qin Z, Li D, Ou Y, et al. Recent advances in polydopamine for surface modification and enhancement of energetic materials: a mini-review. *Crystals* 2023;13:976.
33. Postma A, Yan Y, Wang Y, Zelikin AN, Tjipto E, Caruso F. Self-polymerization of dopamine as a versatile and robust technique to prepare polymer capsules. *Chem Mater* 2009;21:3042–4.
34. Wang L, Liu J. Dopamine polymerization-mediated surface functionalization toward advanced bacterial therapeutics. *Acc Chem Res* 2024;57:945–56.
35. Feng P, Qiu X, Yang L, et al. Polydopamine constructed interfacial molecular bridge in nano-hydroxylapatite/polycaprolactone composite scaffold. *Colloids Surf B Biointerfaces* 2022;217:112668.
36. Sahiner N, Sagbas S, Sahiner M, Blake DA, Reed WF. Polydopamine particles as nontoxic, blood compatible, antioxidant and drug delivery materials. *Colloids Surf B Biointerfaces* 2018;172:618–26.
37. Liu X, Cao J, Li H, et al. Mussel-inspired polydopamine: a biocompatible and ultrastable coating for nanoparticles in vivo. *ACS Nano* 2013;7:9384–95.
38. Si L, Zhang S, Guo H, et al. Swarming magnetic Fe_3O_4@polydopamine-tannic acid nanorobots: integrating antibiotic-free superficial photothermal and deep chemical strategies for targeted bacterial elimination. *Research* 2024;7:438.
39. Xie L, Liu Y, Zhang W, Xu S. A dopamine/tannic-acid-based co-deposition combined with phytic acid modification to enhance the anti-fouling property of RO membrane. *Membranes (Basel)* 2021;11:342.
40. Zhang H, Shen X, Fei Z, et al. Ag-incorporated polydopamine/tannic acid coating on titanium with enhanced cytocompatible and antibacterial properties. *Front Bioeng Biotechnol* 2022;10:877738.
41. Chen CC, Wang JM, Huang YR, Yu YH, Wu TM, Ding SJ. Synergistic effect of thermoresponsive and photocuring methacrylated chitosan-based hybrid hydrogels for medical applications. *Pharmaceutics* 2023;15:1090.
42. Chung JJ, Chen CC, Ding SJ. Strontium-polydopamine hybrid coating to improve antibacterial ability and osseointegration of titanium implants. *Mater Chem Phys* 2024;312:128629.
43. Li YM, Miao X, Wei ZG, et al. Iron-tannic acid nanocomplexes: facile synthesis and application for removal of methylene blue from aqueous solution. *Dig J Nanomater Biostruct* 2016;11:1045–61.
44. Wu IT, Chu YH, Huang YR, Chen CC, Ding SJ. Antibacterial ability and osteogenic activity of polyphenol-tailored calcium silicate bone cement. *J Mater Chem B* 2022;10:4640–9.
45. Koochakzaei A, Sabaghian M. Tannin characterization and sourcing in historical leathers through FTIR spectroscopy and PCA analysis. *Collag Leat* 2023;5:21.
46. Thakur A, Ranote S, Kumar D, Bhardwaj K, Gupta R, Chauhan G. Synthesis of a PEGylated dopamine ester with enhanced antibacterial and antifungal activity. *ACS Omega* 2018;3:7925–33.
47. Kaczmarek-Szczepańska B. Tannic acid with antiviral and antibacterial activity as a promising component of biomaterials – a minireview. *Materials* 2020;13:3224.
48. Qiu WZ, Yang HC, Xu ZK. Dopamine-assisted co-deposition: an emerging and promising strategy for surface modification. *Adv Colloid Interface Sci* 2018;256:111–25.
49. Guo Q, Chen J, Wang J, Zeng H, Yu J. Recent progress in synthesis and application of mussel-inspired adhesives. *Nanoscale* 2020;12:1307–24.
50. Moorhead A, Francis LF. Characterizing stress development and cracking of ceramic particulate coatings during drying. *J Am Ceram Soc* 2024;107:2837–48.
51. Villanueva X, Zhen L, Ares J, et al. Effect of chemical modifications of tannins on their antimicrobial and antibiofilm effect

against Gram-negative and Gram-positive bacteria. *Front Microbiol* 2023;13:987164.
52. Dai Q, Zong Y, Zhu J, et al. A chronological regulated implant coating with antibacterial and osteogenesis constructed by TA-mediated LbL self-assembly. *Mater Des* 2024;241:112897.
53. Kaczmarek-Szczepańska B, Zasada L, Michalska-Sionkowska M, Vishnu J, Manivasagam G. The modification of titanium surface by decomposition of tannic acid coating. *Appl Sci* 2023;13:5204.
54. Wang J, Zhao R, Cheng Z, Wang P, Jin M, Xu J. An antifouling coating based on tannic acid: an eco-friendly strategy for antioxidant removal of reactive oxygen species. *J Appl Polym Sci* 2025;142:e57227.
55. Cheng F, Yao C, Yi X, Li H, Huang Y, He J. Multifunctional bacterial cellulose-based hydrogel with tannic acid (TA)-modified MXene for antibacterial photothermal therapy and accelerated wound healing. *Int J Biol Macromol* 2025;322:146565.
56. Yang YP, Zhao JQ, Gao HB, et al. Tannic acid alleviates lipopolysaccharide-induced H9C2 cell apoptosis by suppressing reactive oxygen species-mediated endoplasmic reticulum stress. *Mol Med Rep* 2021;24:535.